Title
Quasi-decadal signals of Sahel rainfall and West African monsoon since the mid-twentieth century

Journal
Journal of Geophysical Research: Atmospheres, 118(22)

ISSN
2169-897X

Authors
Dieppois, Bastien
Diedhiou, Arona
Durand, Alain
et al.

Publication Date
2013-11-27

DOI
10.1002/2013jd019681

Peer reviewed

Quasi-decadal signals of Sahel rainfall and West African monsoon since the mid-twentieth century

Bastien Dieppois,[1] Arona Diedhiou,[2] Alain Durand,[1] Matthieu Fournier,[1] Nicolas Massei,[1] David Sebag,[1,3] Yongkang Xue,[4,5] and Bernard Fontaine[6]

Received 20 February 2013; revised 9 November 2013; accepted 11 November 2013.

[1] Sahel rainfall shows pronounced decadal variability and a negative trend between wet conditions in the 1950s–1960s and dry ones in the 1970s–1980s. Using continuous wavelet transform, the quasi-decadal variability (QDV) of rainfall reveals zonal contrasts. The highest QDV is identified in the 1950s–1960s over western Sahel and in the 1970s–1980s over eastern Sahel. The quasi-decadal atmospheric anomalies have been reconstructed using Fourier transform for the 1950s–1960s and the 1970s–1980s, respectively, and assessed by the composite analysis of the QDV phases for the periods before and after 1968. Over western Sahel, the rainfall QDV in the 1950s–1960s is related to the North Atlantic sea surface temperature (SST) variability, as highlighted by the wavelet coherence. A southward shift trend of the Intertropical Convergence Zone (ITCZ) is identified through an enhancement of northeasterly fluxes and moisture convergence over the western part of West Africa. A decrease (increase) of southern (northern) subtropical sinking motions seems to be involved. In the 1970s–1980s, a strengthening of cross-equatorial Atlantic SST and pressure gradients is related to an increase of monsoon flow from lower troposphere up to the midtroposphere and to the northward shift of the ITCZ, mainly over eastern Sahel. The Pacific SST influence is also identified, which involves changes in the global zonal circulation.

Citation: Dieppois, B., A. Diedhiou, A. Durand, M. Fournier, N. Massei, D. Sebag, Y. Xue, and B. Fontaine (2013), Quasi-decadal signals of Sahel rainfall and West African monsoon since the mid-twentieth century, *J. Geophys. Res. Atmos.*, *118*, doi:10.1002/2013JD019681.

1. Introduction

[2] The observed widespread drought in West Africa during the 1970s and 1980s was the most significant drought at the regional scale during the twentieth century [*African Monsoon and Multidisciplinary Analyses International Scientific Steering Committee*, 2005]. The associated decadal rainfall variability has been associated with the effect of three competing factors which contribute differently in the interhemispheric sea surface temperature (SST) signature [*Mohino et al.*, 2011]: a multidecadal warming trend of the global SSTs and two patterns of decadal variability in the Atlantic Multidecadal Oscillation and the Interdecadal Pacific Oscillation. Moreover, decadal rainfall variability could be related to the occurrence of individual rainy systems [*Le Barbé and Lebel*, 1997] and is part of complex multiple-scale interactions between convection and large-scale dynamics characterizing the West African monsoon (WAM) [*Redelsperger et al.*, 2002].

[3] The documented spatiotemporal variability of rainfall in West Africa is related to convection processes [e.g., *Janicot*, 1992; *Rodwell and Hoskins*, 1996]. In particular, it has been shown that 80% of Sahel rainfall is associated with organized deep convective systems called "mesoscale convective systems" (MCSs) [*Mathon and Laurent*, 2001]. Two key convective patterns of the WAM dynamics result from the convergence of the northerly Harmattan and the southwesterly monsoon flows along the intertropical discontinuity (ITD) [*Peyrille et al.*, 2007]: (1) the Intertropical Convergence Zone (ITCZ) corresponding to deep wet convection and (2) the Saharan Heat Low corresponding to deep dry convection. This meridional circulation is coupled with a zonal circulation characterized by two major jets: the Tropical Easterly Jet (TEJ), at 200 hPa, closely related to the deep wet convection; the African Easterly Jet (AEJ), at 600 hPa, which provides the instability for the growth of African easterly waves [*Burpee*, 1972; *Reed et al.*, 1977;

[1]Laboratoire Morphodynamique Continentale et Côtière, Université de Rouen, CNRS, Mont-Saint Aignan, France.
[2]Laboratoire d'étude des Transferts en Hydrologie et Environnement, Université de Grenoble, IRD, Grenoble, France.
[3]Laboratoire HydroSciences Montpellier, Université de Montpellier 2, IRD, Montpellier, France.
[4]Department of Geography, University of California, Los Angeles, California, USA.
[5]Department of Atmospheric and Oceanic Sciences, University of California, Los Angeles, California, USA.
[6]Centre de Recherches en Climatologie, Université de Bourgogne, CNRS, Dijon, France.

Corresponding author: B. Dieppois, Laboratoire Morphodynamique Continentale et Côtière, UMR 6143, CNRS/Université de Rouen, FED 4116 SCALE, Place Emile Blondel, FR-76821 Mont-Saint Agnan, France. (bastien.dieppois@univ-rouen.fr)

2169-897X/13/10.1002/2013JD019681

Western Sahel

Stations	Country	Coordinates	Record period
Dakar	Senegal	14.7N, 17.5W, 24m	1897-2010
St-Louis	Senegal	16.1N, 16.5W, 4m	1854-2010
Kaolack	Senegal	14.9N, 16.07W, 25m	1918-2003
Linguère	Senegal	15.4N, 15.1W, 21m	1934-2003
Matam	Senegal	15.6N, 13.3W, 15m	1922-2003
Bakel	Senegal	14.9N, 12.4W, 25m	1918-2003
Mopti	Mali	14.5N, 4.2W, 271m	1921-2010
Ouahigouya	Burk-Faso	13.6N, 2.4W, 329m	1920-2010

Eastern Sahel

Stations	Country	Coordinates	Record period
Tillaberi	Niger	14.2N, 1.5E, 209m	1923-1997
Niamey	Niger	13.5N, 2.1E, 234m	1905-2010
Tahoua	Niger	14.9N, 5.3E, 386m	1922-2000
Maradi	Niger	13.5N, 7.1E, 368m	1931-2005
Magaria	Niger	13N, 8.9E, 360m	1922-1998
Goure	Niger	14N, 10.3E, 460m	1936-1996
Maine-Soroa	Niger	13.2N, 12E, 338m	1936-2005
Maiduguri	Nigeria	11.9N, 13.1E, 354m	1909-1995
N'Djamena	Chad	12.1N, 15E, 294m	1932-2010

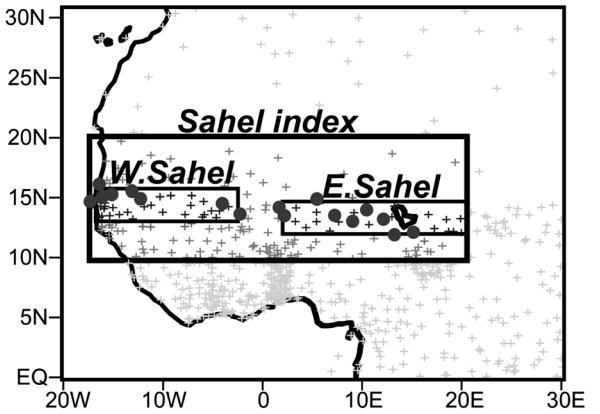

Figure 1. Detailed information and geographical location of selected rainfall stations over western and eastern Sahel. On the map: the bold grey points indicate the Sahel rainfall stations used in Figure 4; the boxes indicate the regions used for defining the rainfall regional indices used in Figures 2 and 4; Plus signs indicate the rainfall station used for defining CRU TS 3.10.1 rainfall fields in West Africa (light grey: the stations used for defining Sahel index; dark grey: the stations used for defining western and eastern Sahel indices).

Leroux and Hall, 2009] and MCS [*Mohr and Thorncroft*, 2006]. This classic view of the WAM dynamics is closely related to seasonal and interannual time scale research. The research on the decadal variability of the WAM is often focused on the rainfall/SST teleconnection [e.g., *Moron*, 1997; *Bader and Latif*, 2003]. The mechanisms involved in these decadal teleconnections have not yet been investigated, which, consequently, affects the ability of coupled models (Climate Model Intercomparison Project 3 and 5 (CMIP3 and 5)) to produce realistic decadal variability in Sahel rainfall in the twentieth century [*Joly et al*., 2007; *Martin et al*., 2013]. Until now, the total variance of decadal Sahel rainfall variability of the CMIP5 simulations is less than one third of the observed value [*Martin et al*., 2013].

[4] The decadal changes that appeared to be homogeneous in the Sahel are superimposed onto the more widely known climatological north-to-south gradient [e.g., *Dai et al*., 2004]. Meanwhile, the Sahel region (i.e., the entire semiarid region south of the Sahara) has shown zonal contrasts over the last 25 years [*Lebel and Ali*, 2009; *Fontaine et al*., 2011a], as in the future climate changes [*Fontaine et al*., 2011b; *Monerie et al*., 2012]. As mentioned above, it is generally accepted that SSTs played a major role in determining the decadal variability of the WAM. *Ward* [1998] first highlighted stronger Indo-Pacific connections with eastern Sahel and stronger North and tropical Atlantic connections with western Sahel. Subsequent studies highlighted the role of Indian and tropical Pacific SSTs [*Bader and Latif*, 2003] and warmer Mediterranean SSTs [*Fontaine et al*., 2011c] in the east-west contrast of Sahel rainfall.

[5] The objective of this paper is to investigate decadal variability of the WAM dynamics with a focus on zonal contrasts of Sahel rainfall. The decadal variability of monsoon circulation is studied through integrated moisture flux and convergence both around lower (1000–850 hPa) and middle (850–500 hPa) levels of the troposphere during decadal wet and dry phases of western and eastern Sahel rainfall. Then the decadal anomalies of eastern and western meridional and zonal dynamics of the WAM are examined through wind components and specific humidity from the lower to upper troposphere. Finally, based on these results, their teleconnections with the Atlantic, Mediterranean, Indian, and Pacific SSTs are discussed.

2. Data and Methods

2.1. Rainfall Data

[6] The time scale of the Sahel rainfall index (Figures 1 and 2a) is preprocessed using the continuous wavelet transform (CWT) [*Torrence and Compo*, 1998]. Although the global wavelet spectrum highlights two decadal time scales of Sahel rainfall variability (Figure 2b)—quasi-decadal (10–20 years) and multidecadal (>20 years)—it is not representative of time fluctuations for these time scales. According to the local wavelet power spectrum (Morlet wavelet: order 6) analysis (Figure 2c), only the quasi-decadal time scale, marked by high variance after 1950, is significantly above the red noise background spectrum (AR[1] = 0.47) (Figure 2c).

[7] To focus on QDV, each time series is first detrended and then filtered using fast Fourier transform (FFT) according to the significant time scale of the continuous wavelet transform. A 10 to 20 year quasi-decadal band-pass filter is used to filter out any multidecadal or interannual variability at each grid point of rainfall fields in West Africa. A quite similar procedure was already applied to the interannual variability of the WAM by *Joly et al.* [2007].

[8] Over the twentieth century, the quasi-decadal filter reconstructs the north-to-south climatological gradient of West African annual rainfall with a standard deviation around 2.5–3 mm month^{-1} in the Sahel region (Figure 2d). The contribution of QDV, here expressed as a percentage of total variance captured by the FFT filter on the overall precipitation variability, is about 0.39% or 8–12% using monthly or annual data. However, east-west contrasts, which will be developed in section 3, are identified in analyzing the spatiotemporal fluctuations of QDV (Figure 2d).

[9] In order to examine the zonal contrasts of Sahel rainfall, western and eastern rainfall indices were computed from the climatic research unit time series 3.10.1 (CRU TS 3.10.1) monthly data sets using an average over 13–15°N and 18–2.5°W for western Sahel and 12–14°N and 2–20°E for eastern Sahel (Figure 1). Because very few rain gauges were available over the Sahel to construct this index before the 1940s, monthly precipitation (from Dakar, Senegal to N'Djamena, Chad) from the Global Historical Climatology Network version-2 (GHCN-2) database was used to check the previous western and eastern Sahel rainfall indices (Figure 1).

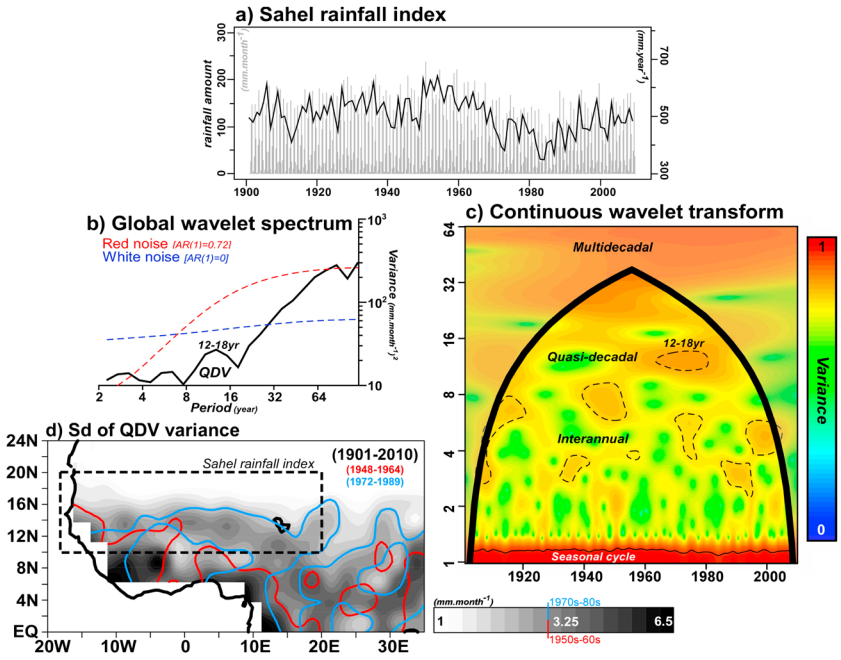

Figure 2. (a) Monthly (grey shaded) and annual (black lines) Sahel rainfall time series used for the spectral analysis. (b) The global wavelet spectrum for the annual Sahel rainfall index (lat: 10–20°N; lon: 20°W–20°E). The dashed red line is the mean red noise spectrum (AR[1] = 0.72), while dashed blue line is the mean white noise spectrum (AR[1] = 0). (c) Wavelet power spectrum of monthly Sahel rainfall index. Bold line (the so-called cone of influence) delineates the area under which power can be underestimated as a result of edge effects, wraparound effects, and zero padding; thin and dashed contour lines show the 90% confidence limits based on 5000 Monte Carlo simulations of the background spectrum AR[1] = 0.47 before and after removal of the seasonal cycle, respectively. (d) Standard deviation of the quasi-decadal Fourier reconstruction of West African rainfall fields at quasi-decadal time scale for period 1901–2010. Bold red and blue contour lines indicate the high amplitude of quasi-decadal variability, i.e., standard deviation larger than 3.25 mm months^{-1} in 1950s–1960s and 1970s–1980s, respectively.

[10] The FFT reconstructions of QDV of monthly Sahel rainfall time series are also compared with reconstructions computed by maximum overlap discrete wavelet transform (MODWT) [*Percival and Walden*, 2000] and by ensemble empirical mode decomposition (EEMD) [*Wu and Huang*, 2009]. The MODWT (using order S8 Symmlet wavelets) which is an undecimated version of the discrete wavelet transform can be regarded as an approximation of the CWT. With the MODWT, time series of nondyadic length can be analyzed, and neither the filter choice nor the starting points of the time series has an influence on the resulting wavelet transform. The EEMD is an autoadaptive, noise-assisted, and data-driven decomposition that extracts internal components of a signal without linear decomposition of reference scales in the initial series and is particularly well adapted to nonstationary intermittent signals.

[11] Finally, the 3 month moving average of western and eastern Sahel rainfall was computed in order to assess the contribution of the QDV at the seasonal scale, expressed as a percentage of total annual rainfall amounts, using the FFT filter. Then these seasonal contributions are compared to the mean annual cycle.

2.2. Atmospheric Data

[12] To identify quasi-decadal signals of WAM since the mid-twentieth century and evaluate the uncertainty in current state-of-the-art data sets, two reanalysis data sets were used. The first is the National Centers for Environmental Prediction/National Center for Atmospheric Research-1 (NNR-1) which is described in detail in *Kalnay et al.* [1996]. *Camberlin et al.* [2001] detected abrupt shifts in NNR-1 geopotential height, temperature, specific humidity, and zonal wind over large parts of tropical Africa around 1967/1968. This artifact may be due to changes in data used for assimilation (e.g., satellite data).

[13] The second data set, the Twentieth Century Reanalysis version 2 (20CR) [*Compo et al.*, 2011], is also introduced for analyses to evaluate the data dependence in this study's results. This is a global reanalysis back in 1850, which has been produced by assimilating only surface pressure observations and using observed SSTs and sea ice concentrations as model boundary conditions.

[14] The moisture flux (Vq) and convergence are integrated over two layers: 1000–850 hPa (i.e., the monsoon layer) and 850–500 hPa (i.e., the AEJ layer) at a quasi-decadal time scale to closely examine the main vertical characteristics of the WAM circulation. This gives a synthetic spatial description of West African monsoon circulation in the low and medium levels of the troposphere at a regional scale, since the moisture flux and divergence take into account wind speed and specific humidity. The western and eastern meridional dynamics from the lower to the upper troposphere (i.e., 1000–300 hPa) are also integrated over meridional cross sections of wind components (v wind and omega) and specific

humidity (q) over the western part (40°S–40°N, 15–5°W) and eastern part (40°S–40°N, 15–5°E), respectively. Finally, a more global perspective of quasi-decadal dynamic anomalies is generated through the zonal cross sections of wind components (u wind and omega) and specific humidity between the Atlantic and Pacific Oceans from the equator to the Sahel (0–20°N, 80°W–180°E).

[15] In each grid point with a 2.5° × 2.5° (2° × 2°) horizontal resolution across 8 (15) vertical levels from 1000 to 300 hPa of NNR-1 (20CR), the time series are subjected to the FFT filter following the method detailed above from 1948 to the present and will be compared to the July–September mean of WAM dynamics in sections 4–6. The latter, however, are only shown using NNR-1 since the patterns are largely similar. There are a number of shortcomings in each data set for the 1948–1957 period [*Stickler and Brönnimann*, 2011]. Due to these shortcomings, which will be introduced in sections 4–6, any identification of quasi-decadal signals of the WAM in this study is validated by cross interpretations of results detected in NNR-1 and 20CR.

2.3. SST Data and Sahel Rainfall Teleconnections

[16] Using the extended reconstructed SST V3b of the National Climatic Data Center [*Smith et al*., 2008], seven regional SST indices were computed as a snapshot of SST evolution since 1901 by averaging the values over (1) the northern Atlantic (NATL: 25–70°N, 7–75°W), the tropical northern and southern Atlantic (TNA: 5–24°N, 50–15°W; TSA: 0–20°S, 30°W–10°E), and the TNA-TSA difference, (2) the whole Mediterranean basin (MED: 29–45°N, 1°W–45°E), and (3) the tropical Indian Ocean (IND: 24°S–24°N, 35–90°E) and the Niño 3.4 region (NIÑO: 5°S–5°N, 170°W–120°W). The time evolution of the quasi-decadal relationships between the Sahel rainfall field and key SST indices is examined using wavelet coherence. Wavelet coherence assesses the linear relationship between two temporal signals $x(t)$ and $y(t)$ around time t_i and scale, with the phase diagram describing the time lag between the signals at any time scale location [*Torrence and Webster*, 1999; *Maraun and Kurths*, 2004]. Similar procedures to those computed for the wavelet spectrum have been conducted to testing covarying power (i.e., 5000 Monte Carlo simulations of two independent AR[1] processes). Processes oscillating on similar frequencies can, however, show patches indicative of an intermittently similar phase evolution. We have, therefore, computed the correlation between quasi-decadal signals of SST and Sahel rainfall indices using a 95% confidence level based on an Ebisuzaki random phase test [*Ebisuzaki*, 1997]. In section 7, we have only displayed an average of quasi-decadal coherence and phase patterns, which are significant at the 90% and 95% confidence level regarding a red noise test and random phase test, in the 1950s–1960s and 1970s–1980s periods.

3. Quasi-Decadal Variability of Eastern/Western Sahel Rainfall

[17] Western and eastern Sahel rainfall indices display strong quasi-decadal signals, which appear significantly above the background red noise (AR[1]: Western Sahel = 0.473; Eastern Sahel = 0.284), as determined by CWT (not shown). These monthly time series (Figure 3a) are then processed with several time scale decompositions. The QDV reconstructed by FFT of both regional Sahel rainfall indices (black lines in Figure 3b) shows standard deviations of 1.6 and 2 mm month^{-1} (including winter months) in western and eastern Sahel, respectively. The standard deviations of the average quasi-decadal scale reconstructions are of the same order using MODWT (1.8 and 2.3 mm month^{-1}) and EEMD (2.2 and 2.1 mm month^{-1}). The QDV based on weather stations is rather high, about 2–5 mm month^{-1}. Figure 3b illustrates the time evolution of rainfall QDV over the Sahel for the twentieth century. Following the local singularities detected by CWT, periods of high-amplitude fluctuations of the rainfall QDV are detected by the FFT band-pass filter, MODWT, and the EEMD (Figure 3b). These three methods produce quite consistent results. In western Sahel (Figure 3b1), QDV signals are reinforced during the 1940–1960 period, and the contribution can range between −9 and 10 mm month^{-1} (based on weather stations). This reinforcement of QDV signals is related to wet conditions in the 1948–1954 (W1) and the 1962–1968 (W2) periods, while dry conditions are observed in the 1940s and the 1955–1961 (D1) periods (Figure 3b). Furthermore, a significant phase shift of western Sahel QDV signals of about 2–4 years is noted due to the small number of available weather stations before the 1940s (Figure 3b). In eastern Sahel (Figure 3a2), the QDV signals are reinforced in the 1970s–1980s, and the contribution can range between −9 and 9 mm month^{-1} (based on weather stations). This reinforcement of QDV signals is associated with wet conditions in the 1975–1981 (W3) and the 1987–1992 (W4) periods, while dry conditions are observed in the 1969–1974 (D2) and the 1982–1987 (D3) periods (Figure 3b2).

[18] The contribution of QDV is not constant during the year and can reach more than 10% of the annual rainfall amount (Figure 3c). During the main rainy seasons of western Sahel (shaded blue), QDV contributes a substantial proportion from August to October (with a peak in September) (black line in Figure 3c1). In eastern Sahel, the seasonal contribution of QDV is more consistent with the rainy season with the largest contribution from June to September (with a peak in July) (Figure 3c2). Regarding the key phases of the annual progression of WAM, the reader is referred to *Thorncroft et al*. [2011]. QDV shows peaks of contribution during the withdrawal phases of the ITCZ in the western Sahel and during the period when the ITCZ moves northward and in the eastern Sahel (Figure 3c).

4. Quasi-Decadal Anomalies of Moisture Flux Convergence Within the Lower and Midtroposphere

[19] This section presents the quasi-decadal signals using differences of wet and dry life cycles of QDV for both periods before and after 1968 in the western Sahel and the eastern Sahel regions. The composites were examined for the following cycles (Figure 3b): during the 1950s and 1960s, the wet life cycles: W1 (1948–1954) and W2 (1962–1968) and dry life cycle: D1 (1955–1961); during the 1970s and 1980s, the wet life cycles: W3 (1975–1981) and W4 (1988–1993) and dry cycles: D2 (1969–1974) and D3 (1982–1987).

[20] In summer, the lower troposphere displays an enhanced southwesterly moisture flux from the Santa Helena

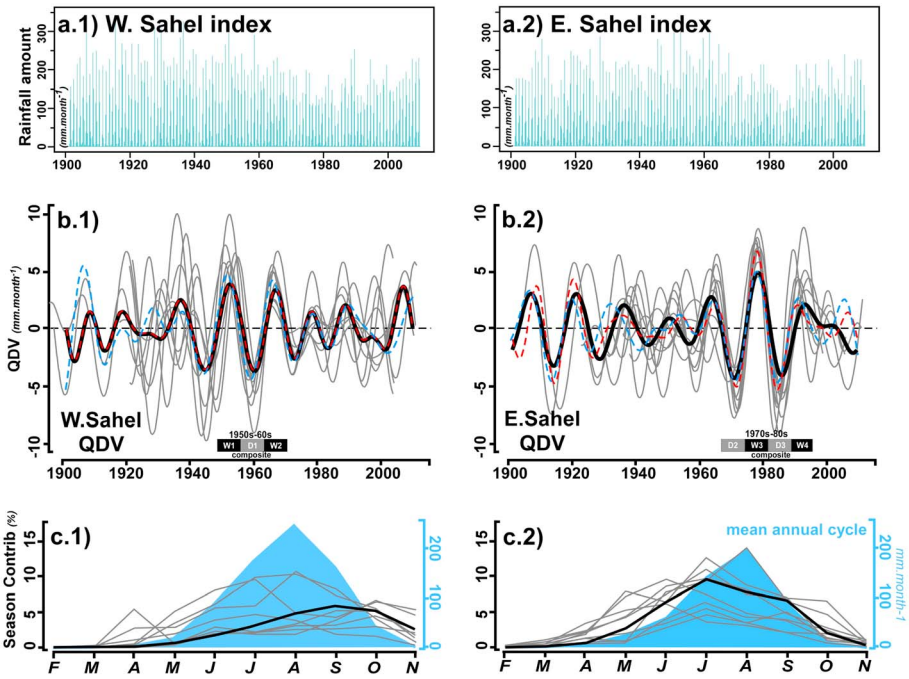

Figure 3. (a). Monthly western and eastern Sahel rainfall time series (shaded blue) used for the spectral decomposition. (b) Quasi-decadal reconstruction of (b1) western and (b2) eastern Sahel rainfall variability (mm month^{-1}) computed by FFT (black line), MODWT (dashed red line), and EEMD (dashed blue line). (c) Seasonal contribution of the (c1) western and (c2) eastern QDV to annual cycle captured by the FFT filter. Comparison between annual cycle (shaded blue) and quasi-decadal rainfall variability is expressed as a percentage of annual rainfall amounts. On all panels, black and grey lines refer to the average of all reconstructions (Sahel rainfall indices plus rain gauges) performed by FFT and selected rain gauges, respectively.

High (Figure 4a1). In the Northern Hemisphere, the southwesterly (monsoon) flux provides the required moisture for the formation of convective clouds over the Sahel region (Figure 4a1). Meanwhile, the northeasterly (Harmattan) flux from the eastern Mediterranean is also strengthened (Figure 4a1). The convergence of these two opposite low-level flows is linked to the ITD (Figure 4a1). The summer ITD is located at the 19°N latitude over western Sahel (18°W–8°E) and 15°N farther east (8–35°E; Figure 4a1).

[21] Figure 4b1 illustrates the difference between the wet and dry quasi-decadal anomalies in the lower troposphere, during high QDV periods of western Sahel rainfall (i.e., W1 + W2 versus D1) in NNR-1 and 20CR. The statistical significance of the differences is estimated on zonal and meridional moisture flux components and convergence using a Student's t test at $p = 0.05$. A significant enhancement of northeasterly moisture flux is detected over the western flank within 5–20°W (Figure 4b1). Meanwhile, using NNR-1, the eastward monsoon flux is enhanced significantly east of Lake Chad (12–35°E) around 10–30°N (Figure 4b1). The 20CR is not consistent with NNR-1 over the eastern regions since the increase of the monsoon flow appears to be considerably shifted farther to the east when using NNR-1 (Figure 4b1). During the 1950s and 1960s, the moisture flux convergence differences are not significant at the 95% confidence level. In Figure 4b1, we multiply the convergence by 300 to be clearly visible. We note that the low-level moisture convergence is slightly enhanced near the Sudano-Guinean and Sahelian zones over the western flank (5–15°N, 18W–2°W; Figure 4b1). This suggests a southward shift trend of the ITD over the western side of West Africa (~9° farther south) (Figure 4b1).

[22] Figure 4c1 illustrates the difference between the wet and dry quasi-decadal anomalies in the lower troposphere, during high QDV periods of eastern Sahel rainfall (i.e., W3 + W4 versus D2 + D3) using NNR-1 and 20CR. During 1970s and 1980s, the quasi-decadal signals are consistent between the two reanalyses (Figure 4c1). An enhancement of low-level monsoon flux is identified over a large part of West Africa (Figure 4c1). A significant enhancement of northeasterly flux is detected over the western flank (18–2.5°W) (Figure 4c1). At the same time, the moisture convergence differences are not statistically significant in the lower troposphere (Figure 4c1). The moisture convergence (divergence) is slightly enhanced throughout the Sahel (Sudano-Guinean zone) and more particularly in the eastern regions (5–25°E) (Figure 4c1). Thus, the ITD tends to be shifted northward over eastern Sahel (~5° or 10° farther north, respectively, using NNR-1 or 20CR; Figure 4c1).

[23] In the midtroposphere, the main divergence and convergence areas during the summer are located, respectively, over the Sahelian and Sudano-Guinean zones (Figure 4a2). The divergence area is associated with the AEJ, which exports atmospheric moisture from the Sahel toward the Atlantic Ocean (Figure 4a2). Because of strong vertical wind shear induced under the AEJ core, the convergence area is related to the deep moist convection process; i.e., the ITCZ is located southward of the jet axis (Figure 4a2).

[24] Figure 4b2 illustrates the difference between wet and dry quasi-decadal anomalies in the midtroposphere in the

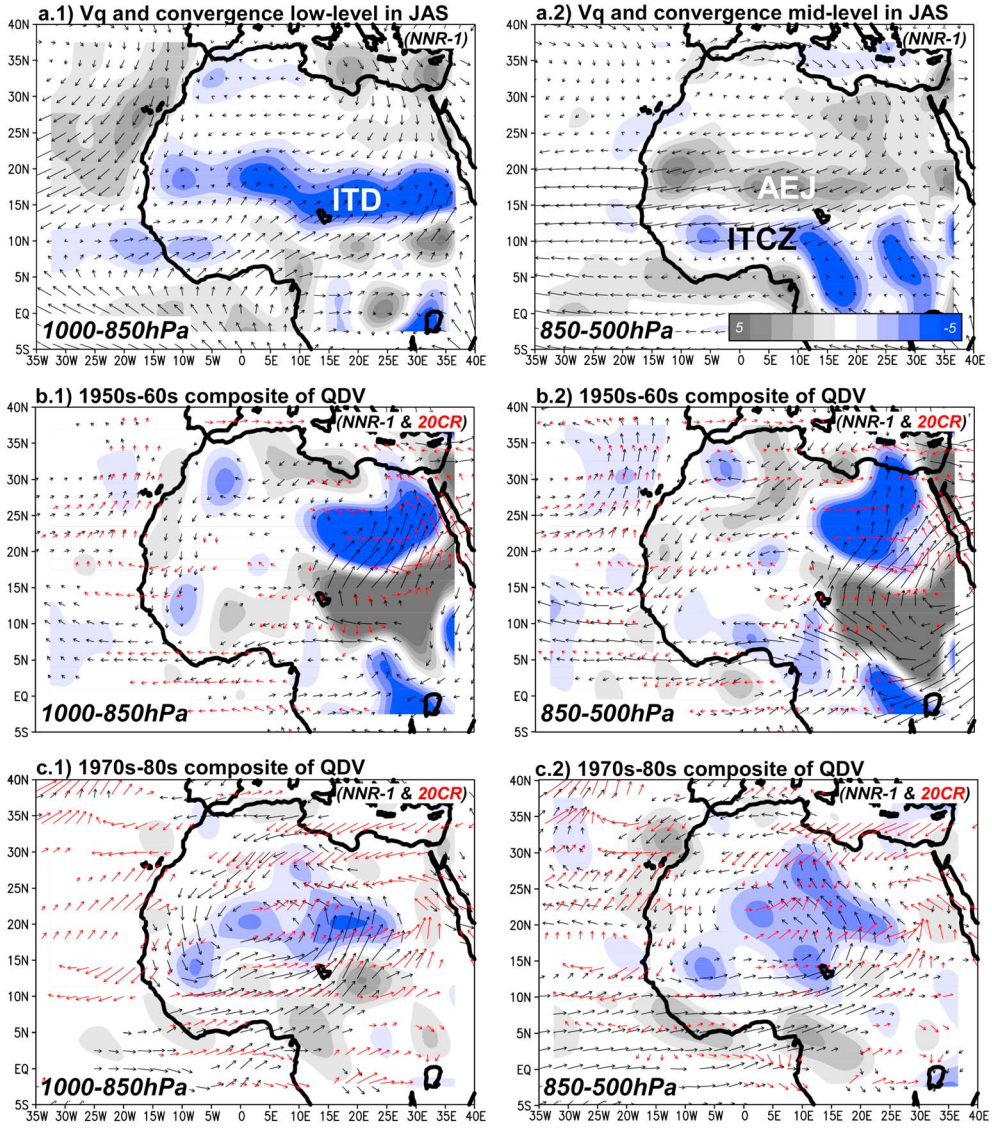

Figure 4. (a) July–September mean integrated moisture fluxes (arrows, in $g\,kg^{-1}\,m\,s^{-1}$) and divergence (shaded blue (grey): convergence (divergence) fields (in $g\,kg^{-1}\,s^{-1}$) in (a1) low troposphere and (a2) midtroposhere using NNR-1). (b and c) Significant differences of quasi-decadal integrated moisture fluxes and convergence fields in (b1 and c1) the low troposphere and (b2 and c2) midtroposphere of NNR-1 and 20CR for 1950s–1960s (W1 + W2 minus D1; Figures 4b1 and 4b2) and 1970s–1980s (W3 + W4 minus D2 + D3; Figures 4c1 and 4c2), respectively. Black and red arrows show the integrated moisture fluxes of NNR-1 and 20CR. The statistical significance of differences has been estimated on zonal and meridional moisture fluxes and convergence using a Student's *t* test at $p = 0.05$. Note: the moisture flux convergence is multiplied by 300 and is not shown for the 20CR for display purpose.

1950s–1960s (i.e., W1 + W2 versus D1), which is characterized by high QDV amplitudes of western Sahel rainfall. A significant enhancement of northeasterly moisture flux is identified using NNR-1 and 20CR over western Sahara and western part of West Africa, although moisture convergence differences are not statistically significant at the 95% confidence level (Figure 4b2). In both reanalyses, an enhancement of midlevel moisture convergence (divergence) is detected around 10°W–15°E (18–10°W) between about 5°N and 25°N (Figure 4b2). Over West Africa, the quasi-decadal signals reveal, therefore, a southward shift trend of the ITCZ. In the midtroposphere, quasi-decadal anomalies are not consistent in these two reanalyses over the eastern regions (Figure 4b2). The differences between NNR-1 and 20CR will be examined in the following section.

[25] Figure 4c2 illustrates the difference between wet and dry quasi-decadal anomalies in the midtroposphere, during high QDV period of eastern Sahel rainfall (i.e., W3 + W4 versus D2 + D3). As in the lower troposphere, quasi-decadal patterns are consistent between NNR-1 and 20CR during this period. The northeastern flux increases in the western region, while a significant enhancement of the southwestern flux is detected over eastern Sahel (Figure 4c2). Such quasi-decadal could be associated with two atmospheric processes: (1)

during a wet summer, the AEJ speed decreases [*Newell and Kidson*, 1984; *Fontaine et al*., 1995; *Grist and Nicholson*, 2001] and (2) the westerly flow extends well into the midtroposphere during the wet anomalies and accounts for the northward shift trend of the AEJ [*Nicholson and Webster*, 2007]. Although this is not significant, the moisture convergence (divergence) is enhanced in the midtroposphere over the Sahel (Sudano-Guinean zone) (Figure 4c2). According to *Tourre et al*. [2010], a strong cross-equatorial pressure gradient is detected since both Atlantic subtropical highs are significantly intensified (Santa Helena High not displayed; Figure 4c2). This is consistent with a development of an equatorial westerly jet; south of the Sahel appears to be dependent on the surface pressure gradient over the tropical Atlantic in accordance with *Thomas and Webster* [1997]. As a result, the ITCZ tends to be shifted northward throughout West Africa (~10° and 15° farther north, respectively, in NNR-1 and 20CR) and especially over the eastern regions (Figure 4c2).

5. Quasi-Decadal Anomalies in Meridional Circulation

[26] The summer meridional circulations present several similarities over the western (15–5°W) and eastern (5–15°E) cross sections from 1948 to 2012 (Figure 5a). NNR-1 is used for Figure 5a. The results of 20CR are not shown since the patterns are largely similar. Both cross sections are marked by a zone of rising motions between the equator and 22°N, which reaches the free troposphere at only around 5–15°N, flanked by two overturning cells linked to Hadley circulation dynamics (Figure 5a). The sinking branch of the southern (northern) cell is around 30–20°S (25–45°N), while its low-level branch is associated with southwesterly monsoon flow (northeasterly circulation) (Figure 5a). The convergence zone between the southern and northern overturning cells defines the ITD and the ITCZ at the surface and in the free troposphere, respectively (Figure 5a). Note that the ITCZ is southward of the ITD (~10° farther south; Figure 5a).

[27] Figures 5b1 and 5b2 illustrate the significant difference between the wet-dry quasi-decadal anomalies of the meridional circulation (integrated V and q) during the high QDV period of western Sahel rainfall (i.e., W1 + W2 versus D1) for 15–5°W and 5–15°E, respectively. Dashed bold lines display only the significant anomalies above 300 g kg^{-1} for the 20CR. However, because NNR-1 humidity difference is not consistent with 20CR, we will mainly focus on wind differences in the following discussion. We note common wind anomalies using NNR-1 and 20CR (Figure 5b1): (1) a decrease of sinking motions between 1000 hPa and 300 hPa over the South Atlantic Ocean, especially between the equator and 20°S, (2) an enhancement (diminution) of northern subtropical sinking motions from 20 to 30°N (30 to 40°N), and (3) an abnormal southern location of the ITCZ (i.e., rising motion and wet anomaly) over the tropical South Atlantic between 10°S and 5°N. However, there are inconsistencies of QDV of western Sahel rainfall when using the two reanalyses. In NNR-1, the increase of northern subtropical sinking motions is associated with reinforcements of low-level northerlies, rising motions above 900 hPa and a wet anomaly over the western Sahel (Figure 5b1). In 20CR, and as a result of underestimations of the northerlies from 900 to 600 hPa along the Atlantic coastal regions between 1948 and 1957 [*Stickler and Brönnimann*, 2011], such anomalies are not identified (Figure 5b1). However, only the results of NNR-1 are in phase with the western Sahel rainfall QDV.

[28] During the same period over the eastern meridional circulation (5–15°E), both reanalyses show significant decreases (increases) of southern subtropical sinking motions around 40–20°S (20–10°S), respectively (Figure 5b2). These two reanalyses reveal different quasi-decadal signals. However, this might be due to overestimations of southwesterlies in NNR-1 over the eastern part of West Africa in the 1950s [*Stickler and Brönnimann*, 2011]. In NNR-1, an enhancement of southwesterly flow, which is likely to drive a northward shift of the ITCZ, is thus identified from 15°S to the Sahel region and can reach the midtroposphere (within 700–500 hPa) above the equator (Figure 5b2). In 20CR, as for the western cross section (Figures 5b1 and 5b2), the quasi-decadal signals reflect a southward shift of the ITCZ leading to a reduction of atmospheric moisture over eastern Sahel (Figure 5b2), which is more consistent with the low QDV of eastern Sahel rainfall during this period.

[29] During the 1970s and 1980s, the meridional circulations are generally similar in both reanalyses (20CR humidity is not shown for better legibility) as determined by the difference between the wet and dry quasi-decadal anomalies (i.e., W3 + W4 versus D2 + D3; Figures 5c1 and 5c2). The two cross sections (i.e., western: 15–5°W; eastern: 5–15°E) show different features. Northern subtropical sinking motions are stronger on the west side, while monsoon flow became stronger on the east side. According to Figure 3a, the atmospheric quasi-decadal signals, nevertheless, are clearer on the eastern cross section (Figures 5c1 and 5c2). A significant increase of southern subtropical sinking motions is identified around 40–20°S (Figure 5c2). The low-level southwesterly flow enhances significantly from 20°S to the equator (Figure 5c2). Over the Sudano-Guinean zone, rising motions and atmospheric moisture are significantly reduced (Figure 5c2). In the Sahel, rising motions and moisture increase significantly up to 600 hPa (Figure 5c1). The northern subtropical sinking motions are also strengthened (Figure 5c1). According to Figures 4c1 and 4c2, the moisture convergence increases (decreases) throughout the Sahel (Sudano-Guinean zone) but is more pronounced over eastern Sahel (Figure 5c). This quasi-decadal pattern is therefore related to a northward shift of the ITCZ (Figure 5c).

[30] In summary, quasi-decadal anomalies show different patterns in meridional circulation before and after 1968 and over the eastern and western flanks. In the 1950s and 1960s, the anomaly of meridional circulation is not fully understood due to lack of consistent results between NNR-1 and 20CR, but, over the western side of West Africa, we can identify a southward/northward (positive/negative phase) shift of the ITCZ. The latter might be associated with a decrease (increase) of the southern (northern) Hadley cell intensity at a regional scale over the western part of West Africa. The 1970s and 1980s periods show a latitudinal shift of the ITCZ related to an intensification of the cross-equatorial pressure gradient and Hadley circulation stronger on the eastern side than on the western side of West Africa.

6. Quasi-Decadal Anomalies in Zonal Circulation

[31] The east-west-oriented Walker circulation is a zonal atmospheric response to zonal thermal contrasts near the

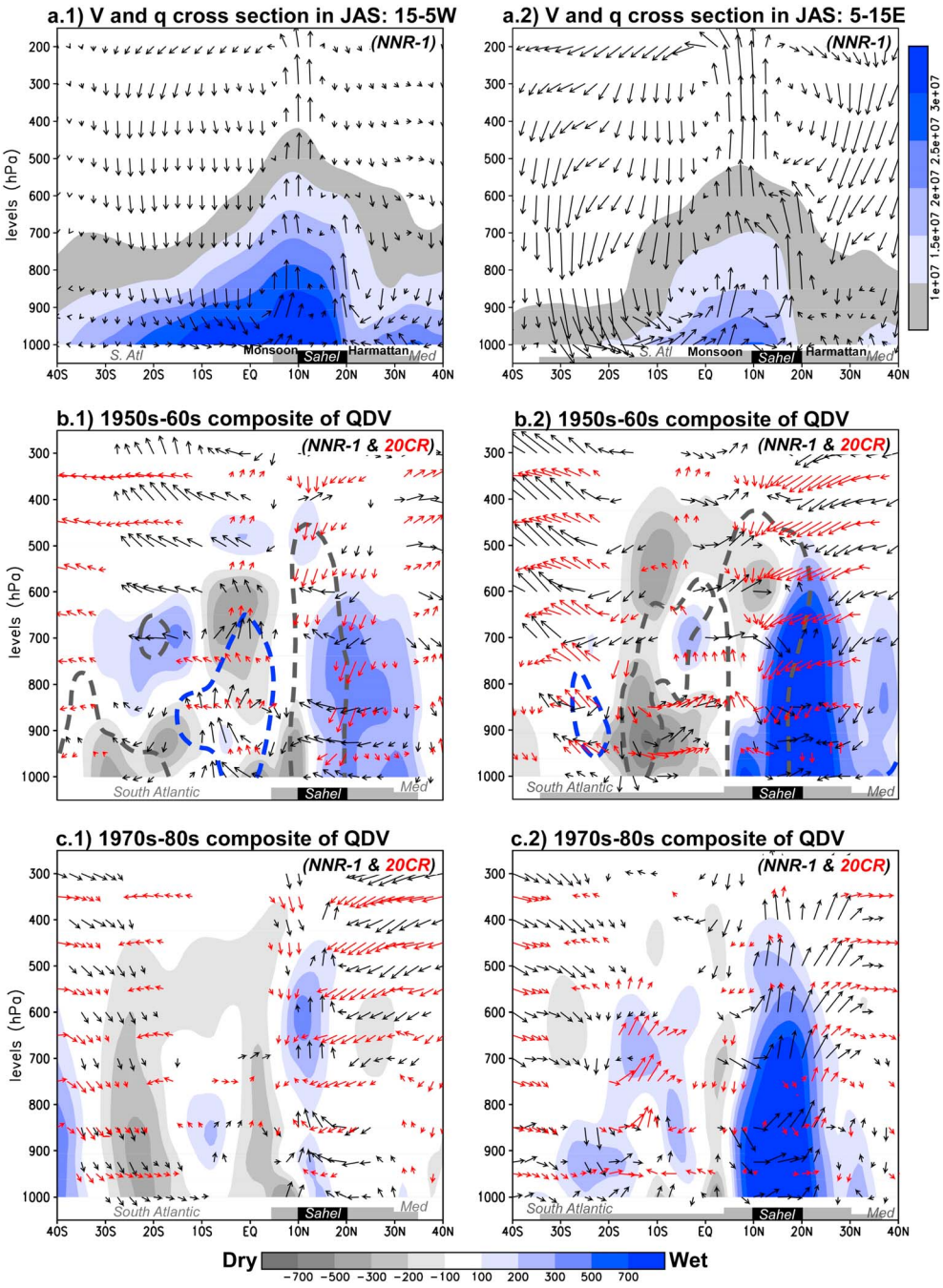

Figure 5. (a) July–September mean of (a1) western (15–5°W) and (a2) eastern (5–15°E) integrated vertical-meridional cross sections of wind (arrows; in m s^{-1}) and atmospheric moisture fields (shaded; in g kg^{-1}) using NNR-1. (b and c) Significant differences of quasi-decadal anomalies of (b1 and c1) western and (b2 and c2) eastern integrated vertical-meridional cross sections of wind and atmospheric moisture fields of NNR-1 (wind: black arrows; humidity: shaded) and the 20CR (wind: red arrows; humidity: dashed bold lines) during the 1950s–1960s (W1 + W2 minus D1; Figures 5b1 and 5b2) and 1970s–1980s (W3 + W4 minus D2 + D3; Figures 5c1 and 5c2). The statistical significance of differences has been estimated on zonal and vertical wind components and moisture using a Student's t test at $p = 0.05$. Note: vertical velocity is multiplied by 200 to be clearly displayed.

equator. Generally, any evolution of the zonal circulation influences the WAM through the generation of anomalies of subsidence and air ascents [*Caminade and Terray*, 2010]. This could explain part of the decadal rainfall variability observed in the dry 1970s and 1980s or since the mid-1990s associated with the zonal recovery of Sahel rainfall [*Hagos and Cook*, 2008]. Figure 6a displays the summer average of the zonal circulation around 0–20°N (V and q). In summer, over the Pacific, the Walker circulation intensifies and becomes well defined, with a branch of strong ascendance concentrated

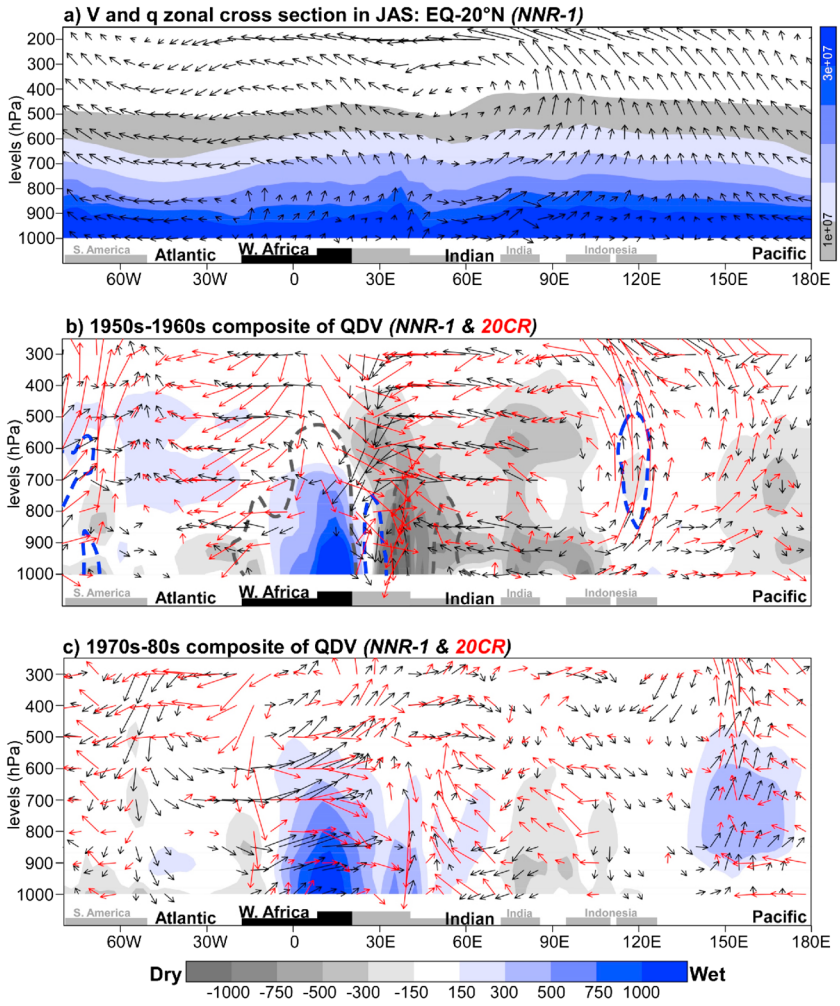

Figure 6. (a) July–September mean of integrated vertical-zonal cross sections of wind (arrows; in m s^{-1}) and atmospheric moisture fields (shaded; in g kg^{-1}) from the equator to 20°N using NNR-1. (b and c) Significant differences of quasi-decadal anomalies of integrated vertical-zonal cross sections of wind and moisture fields of NNR-1 (wind: black arrows; humidity: shaded) and 20CR (wind: red arrows; humidity: dashed bold lines) during the 1950s–1960s (W1 + W2 minus D1; Figure 6b) and 1970s–1980s (W3 + W4 minus D2 + D3; Figure 6c). The statistical significance of differences has been estimated on zonal and vertical wind components and atmospheric moisture regarding a Student's t test at $p = 0.05$. Note: vertical velocity is multiplied by 150 to be clearly displayed.

near 130°E (warm pool region), and midtroposphere sinking motions are found over the western Indian Ocean around 48–58°E (Figure 6a). These sinking motions are connected by low-level westerly wind blowing from the Indian Ocean toward the western Pacific, joining the Pacific rising branch. Thus, the overturning is completed by the returning upper-level easterlies over the Indian Ocean to the Atlantic sinking branch (Figure 6a). In West Africa, two secondary zonal cells between the Atlantic and Indian Oceans are related to rising motions up to the free troposphere (Figure 6a), which generates deep moist convection processes.

[32] Figure 6b displays the difference between the wet and dry quasi-decadal anomalies of the integrated zonal circulation (V and q) around 0–20°N in the 1950s–1960s (i.e., W1 + W2 versus D1) in both reanalyses. As a reminder, this period is characterized by high QDV amplitudes of rainfall over the western Sahel (Figure 3a1). Because the NNR-1 humidity difference is not consistent with 20CR, dashed bold lines display only the significant anomalies above 300 g kg^{-1} for 20CR. Over the Pacific Ocean, a significant decrease (increase) of rising motions and atmospheric moisture is detected around 150–180°E (130–150°E), which suggests a westward shift of the rising branch of the Pacific overturning cell, hence the increase of rising motions over South America observed in both reanalyses (Figure 6b). A significant reduction of moisture and a few decadal wind anomalies are common in both reanalyses over the Indian Ocean (Figure 6b): (1) rising motion increases around 105–130°E, (2) the upper level easterly wind increases, and (3) both low-level rising motion and middle- to upper level sinking motion increase over the western Indian Ocean and eastern Africa. The Walker circulation is therefore intensified over the Indian and Pacific Oceans. Meanwhile, in both reanalyses, very few quasi-decadal signals are significantly detected in the Walker circulation around 1000–850 hPa over West Africa. Differences of QDV signals are nonetheless identified

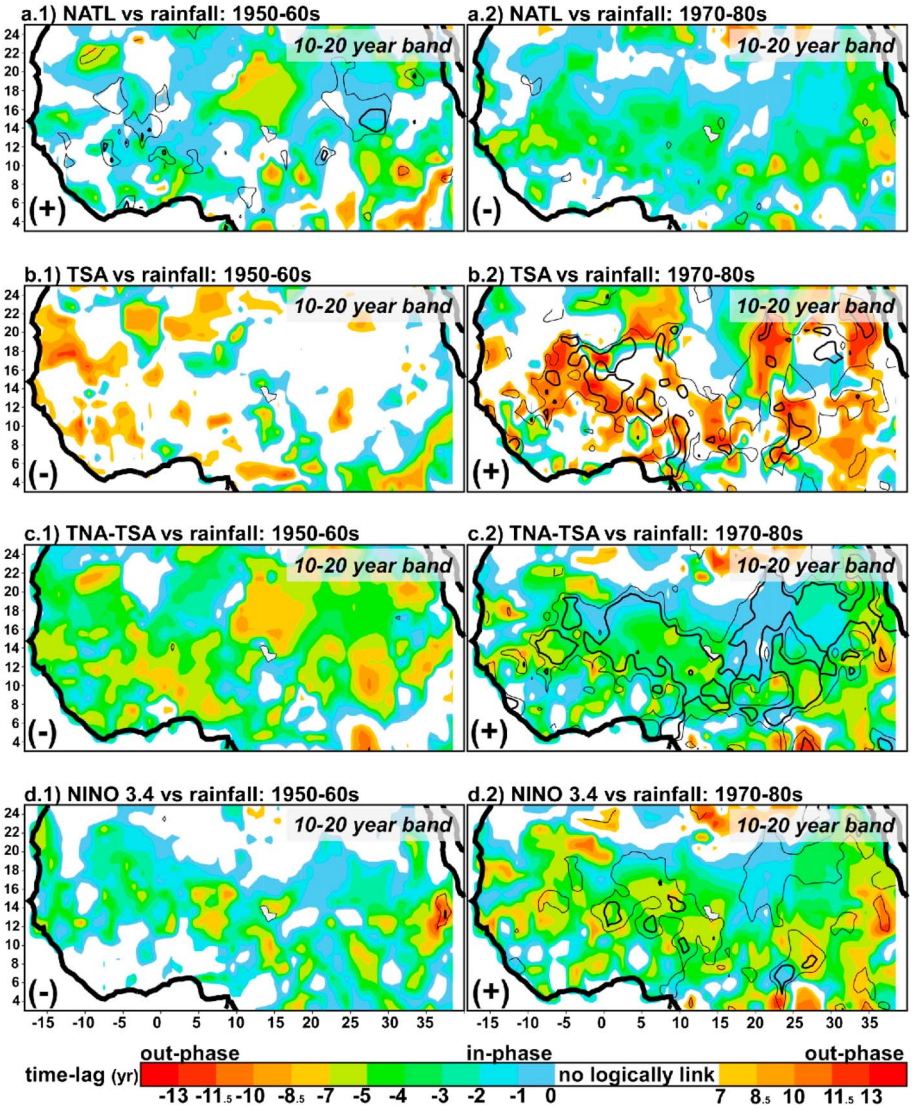

Figure 7. (left column) Quasi-decadal patterns (10–20 year) of the wavelet coherence (contour) and phase (shaded) between West African rainfall fields and selected SST indices ((a) NATL; (b) TSA; (c) TNA-TSA; (d) NIÑO 3.4) (10–20 year) in the period 1950s–1960s. (right column) The period 1970s–1980s. Thin and thick contours, respectively, refer to significant coherence performed by Monte Carlo simulations at the 90% and 95% confidence limits. Positive time lag is masked due to the weakness of logical interpretations.

over the African continent, but, compared to upper air observations in the 1950s, 20CR shows larger deviations than NNR-1 over the Africa-Asia longitudinal window [*Stickler and Brönnimann*, 2010]; and the quasi-decadal anomalies of 20CR are out of phase with western Sahel rainfall QDV. NNR-1 pattern appears more consistent and shows an increase of rising motions (above 700 hPa) and atmospheric moisture from 15°W to 10°E.

[33] In the 1970s–1980s, the quasi-decadal signals of the integrated zonal circulation are also determined around 0–20°N using the difference of wet and dry life cycles during a period of high QDV variance of rainfall in the eastern Sahel (i.e., W3 + W4 versus D2 + D3; Figure 6c). The results of NNR-1 and 20CR are highly consistent for this period; therefore, the 20CR humidity is not shown. Over the Pacific Ocean, a significant increase (decrease) of rising motions and atmospheric moisture is identified around 140–180°E (120–140°E). An eastward shift of the Pacific overturning cell could therefore be involved (Figure 6c). Over the Indian Ocean, we observe significant anomalies between the 1970s and 1980s (Figure 6c): (1) within 40–80°E, a decrease of low-level westerly wind and upper level easterly wind and (2) both low-level rising and middle- to upper level sinking motions decrease over the western Indian Ocean and eastern Africa. These wind anomalies are related to a weakening of the Walker circulation over the Indian and western Pacific Oceans (Figure 6c). Over the Atlantic Ocean, an increase of sinking motions is identified around 60–10°W in NNR-1 and is located slightly farther east in 20CR (20–10°W), hence the decrease of atmospheric moisture over western Sahel and the low QDV signal (Figure 6c). Farther east, i.e., over West Africa, significant increases of rising motions and atmospheric moisture and a decrease of easterly winds are detected, resulting in an increase of the atmospheric moisture

and the QDV signal of eastern Sahel rainfall (Figure 6c). This latter anomaly is also consistent with a decrease of easterly wind components in the middle and upper tropospheres, i.e., in the AEJ and the TEJ layers (Figure 6c).

7. Time Evolution of SST Teleconnections

[34] Figure 7 shows significant results of wavelet coherence and phase applied to key SST indices and West African rainfall fields. At the quasi-decadal time scale, the coherence of rainfall with Mediterranean, Indian, and tropical North Atlantic SSTs is rejected at the 90% and 95% confidence level using a red noise test or random phase test (not shown). The time evolution of rainfall/SST teleconnections displays zonal contrasts at this scale, which can be fully associated with various WAM anomalies.

[35] In the 1950s–1960s, the quasi-decadal covarying power between the Sahelian rainfall field and the SST indices is only significant within the extratropical North Atlantic SST (NATL), especially over western Sahel and eastward of Lake Chad (Figure 7a1). Quasi-decadal coherence patterns of NATL and Sahel rainfall are in phase. Enhanced rainfall over the Sahel is related to the positive phase of NATL in accordance with previous studies [e.g., *Folland et al*., 1986; *Zhang and Delworth*, 2006]. Moreover, NATL mainly leads the statistical relationship from a −3 year to +1 year lag (Figure 7a1). Although this relationship remains weak, they can be partly related to quasi-decadal atmospheric anomalies already detected in NNR-1 and 20CR over the western flank of West Africa as well as eastward of Lake Chad (Figures 4–7). This might imply changes in both the meridional and zonal cell circulations over monsoon regions, although this cannot be directly proved here. Indeed, inconsistencies between the results of NNR-1 and 20CR make interpretations very difficult. Nevertheless, in the 1950s–1960s, an overview of anomalies points to a large-scale relationship impacting both the African and Indian longitudinal windows, since at the quasi-decadal time scale, NATL variability contributes to regulating a significant part of the mean cross-hemispheric temperature gradient, which controls the northward penetration of the monsoon in these regions.

[36] At the quasi-decadal time scales, both tropical Atlantic (TSA, TNA − TSA) and Pacific (NIÑO 3.4) SST variations are coherent with those recorded in Sahel rainfall, although more strongly across the eastern flank and during the 1970s and 1980s (Figures 7b2–7d2, right column). Tropical South Atlantic SST (TSA) and Sahel rainfall show an out-phase quasi-decadal pattern, in agreement with *Polo et al*. [2008] and *Losada et al*. [2009], showing that warmer (cooler) TSA is related to a decrease (increase) of Sahelian (Sudano-Guinean) convergence and southward (northward) displacement of the ITCZ. Moreover, TSA leads Sahel rainfall by ~2–5 years (Figure 7b2). According to earlier studies [*Allen and Smith*, 1994; *Mehta and Delworth*, 1995; *Moron*, 1997; *Giannini et al*., 2003; *Tourre et al*., 2010], the TNA-TSA and Sahel rainfall relationship reveals an in-phase coherence pattern at the quasi-decadal time scale (Figure 7d2). The SST signal leads Sahel rainfall variability by ~2–4 years (Figure 7c2). Such fluctuations of the thermal gradient over the tropical Atlantic region are thus likely to drive monsoon flow variations and to the development of an equatorial westerly jet around 850–700 hPa, in agreement with the northward/southward shift of the ITCZ (Figures 4–6).

[37] Quasi-decadal fluctuations (~12–20 years) in the Pacific Ocean have been significantly identified using spectral analyses [*Torrence and Webster*, 1999; *Tourre et al*., 2001]. Some aspects of these fluctuations have been modeled [*Pierce et al*., 2001; *Qiu*, 2003] and fully described in *White et al*. [2003] and *Tourre et al*. [2005]. Its characteristics can be seen as an amplitude modulation of El Niño–Southern Oscillation events [*Tourre et al*., 2005]. QDV of Pacific SST (NIÑO 3.4) leads Sahel rainfall from 4 to 7 years (Figure 7d2) but is significant regarding the random phase test (correlation $[r] = 0.3267 >$ probability at the 95 % level $[p] = 0.1605$). The African/Pacific teleconnection is probably modulated by fluctuations affecting the Pacific region versus the Atlantic modes of variability: this changes SST anomalies and modifies the frequency/intensity of atmospheric waves over African regions. According to *Wang* [2001], the NIÑO-like pattern could be associated with a decrease of the Walker circulation over the Indian and an eastward shift of the Pacific overturning cell (Figure 6c). Such induced anomalies would likely to drive an increase of subsidence over the equatorial Atlantic up to western Sahel (reducing the QDV signal in western Sahel rainfall) in agreement with *Mohino et al*. [2011] (Figure 6c).

8. Discussion and Conclusion

[38] The quasi-decadal time scale is detected, and zonal contrasts in Sahel rainfall are displayed. Western Sahel rainfall shows high-variance QDV in the 1950s–1960s, while eastern Sahel rainfall reveals high-amplitude QDV in the 1970s–1980s. This quasi-decadal rainfall variability is consistent with the Sahel rainy season in eastern Sahel but is expressed from August to October in western Sahel.

[39] Across the quasi-decadal time scales, time periods of high QDV variance in both western and eastern Sahel rainfall are examined through quasi-decadal WAM anomalies. In the 1950s and 1960s, quasi-decadal anomalies of WAM are located over the western part of West Africa and eastward to Lake Chad. This pattern, however, is not widely known since it can only be related to the North Atlantic SST. Moreover, during this period, inconsistencies in the results using NNR-1 and 20CR show the relative weakness in the results before 1968, especially over the eastern region. Some consistent quasi-decadal anomalies are nonetheless identified in both reanalyses over the western side of West Africa. The key features of the 1950s–1960s quasi-decadal anomalies in the wet period are (1) an enhancement of a low- to middle-level northeasterly flux and southward/northward variations of the ITCZ, (2) an enhancement of moisture convergence over the western Sahel, (3) a decrease (increase) of southern (northern) subtropical sinking motions, and (4) as shown in NNR-1, an increase of rising motions above 900 hPa and atmospheric moisture advected from the north over the western Sahel. However, the latter should be checked by analysis of quasi-decadal signals using observed upper air data before the 1960s following *Stickler and Brönimann* [2010, 2011], or with atmospheric general circulation model (AGCM) ensemble forced by retrospective SSTs. It should also be noted that these observations must systematically integrate synoptic-, annual-, and interannual-scale interactions since,

physically, most of the atmospheric moisture is contained in the monsoon flow.

[40] In the 1970–1980 wet life cycles, through NNR-1 and 20CR, a strengthening of both cross-equatorial Atlantic SST and pressure gradient can be related to an enhancement of monsoon flow up to the midtroposphere (850–700 hPa) and to moisture convergence, especially over eastern Sahel, therefore implying a northward shift of the ITCZ. Such patterns seem similar to the anomalous inertial instability involved in the development of the African Westerly Jet [*Nicholson and Webster*, 2007], which could therefore play a role at the quasi-decadal time scale. AEJ speed variations could also be supported by the observed zonal circulation anomalies. Nevertheless, the combination of meridional gradients of soil moisture and vegetation properties (including albedo) is also crucial for generating and maintaining the AEJ [*Cook*, 1999; *Wu et al*., 2009]. In this period, the Pacific SSTs could also play a key role in driving the quasi-decadal anomalies of Sahel rainfall. The NIÑO-like pattern can probably be associated with the decrease of the Walker circulation over the Indian Ocean and of the eastward shift of the Pacific rising branch. These fluctuations can contribute to an increase of subsidence over the equatorial Atlantic up to the western side of the African continent, hence the low QDV in western Sahel rainfall. Another important aspect of 1970s–1980s anomalies is the decrease of easterly wind components at TEJ levels and the associated divergence in the high troposphere. This suggests a reduction of the deep wet convection activity over WAM and in the Indian monsoon region, although this cannot be proved here [*Sathiyamoorthy et al*., 2007].

[41] This study explores the Sahel rainfall decadal variability and its associations with zonal contrasts through an investigation of decadal WAM variability and SST forcing. As described by *Jury* [2010], the interaction of Walker and Hadley cells over Africa appears to be a key feature that modulates climate at decadal frequency through anomalous north-south displacement of the near-equatorial trough. However, SST forcing is not the only factor impacting both decadal variability of Sahel rainfall and WAM. Atmospheric internal variability [*Caminade and Terray*, 2010], global warming [*Paeth and Hense*, 2004], and vegetation feedback processes [*Zeng et al*., 1999] may also contribute substantially to driving decadal to multidecadal rainfall variability. In fact, upcoming investigations will be based on sensitivity experiments focusing on multiple factors and conducted with several AGCMs forced by SSTs such as in the second phase of the West African Monsoon Modeling and Evaluation (WAMME-2) project [*Xue et al*., 2012].

[42] **Acknowledgments.** This study was conducted as part to the CORUS2 project entitled "Impact de la pression anthropique et du changement global sur les flux sédimentaires en zone sahélienne" (grant 6116) supported by the French Institute of Research for Development (Institut de Recherche pour le Développement, IRD). This topic has been a contribution to the AMEDE (Analyse Multi-Echelle de la Dynamique Eolienne au Sahel) action based on the FED 4116 SCALE (TEQQ project) supported by the Upper Normandy region (France), as well as US NSF AGS-1115506. The authors are also grateful to Pr. Mathieu Rouault for his helpful friendly review of the manuscript.

References

Allen, M. R., and L. A. Smith (1994), Investigating the origins and significance of low-frequency modes of climate variability, *Geophys Res Lett*, *21*, 883–886.

African Monsoon and Multidisciplinary Analyses International Scientific Steering Committee (AMMA ISSC) (2005), The international science plan for AMMA. http://www.amma.mediasfrance.org/library/docs/AMMA_ISP_May2005.pdf.

Bader, J., and M. Latif (2003), The impact of decadal-scale Indian Ocean sea surface temperature anomalies on Sahelian rainfall and the North Atlantic Oscillation, *Geophys. Res. Lett.*, *30*(22), 2169, doi:10.1029/2003GL018426.

Burpee, R. W. (1972), The origin and structure of easterly waves in the lower troposphere of North Africa, *J. Atmos. Sci.*, *29*, 77–-90.

Camberlin, P., S. Janicot, and I. Poccard (2001), Seasonality and atmospheric dynamics of teleconnection between African and tropical sea-surface temperature: Atlantic vs. ENSO, *Int. J. Climatol.*, *21*, 973–1005.

Caminade, C., and L. Terray (2010), Twentieth century Sahel rainfall variability as simulated by the ARPEGE AGCM, and futures changes, *Clim. Dyn.*, *35*, 75–94.

Compo, G. P., et al. (2011), The Twentieth Century Reanalysis Project, *Q. J. R. Meteorol. Soc.*, *137*, 1–28.

Cook, K. H. (1999), Generation of the African easterly jet and its role in determining West African precipitation, *J. Clim.*, *12*, 1165–1184.

Dai, A., P. J. Lamb, K. E. Trenberth, M. Hulme, P. D. Jones, and P. Xie (2004), The recent Sahel drought is real, *Int. J. Climatol.*, *24*, 1323–1331.

Ebisuzaki, W. (1997), A method to estimate the statistical significance of a correlation when the data are serially correlated, *J. Clim.*, *10*, 2147–2153.

Folland, C. K., T. N. Palmer, and D. E. Parker (1986), Sahel rainfall worldwide sea temperatures, 1901-85, *Nature*, *320*, 602–606.

Fontaine, B., S. Janicot, and V. Moron (1995), Rainfall anomaly patterns and wind field signals over West Africa in August (1958-1989), *J. Clim.*, *8*, 1503–1510.

Fontaine, B., P. Roucou, M. Gaetani, and R. Marteau (2011a), Recent changes in precipitations, ITCZ convection and northern tropical circulation over North Africa (1979-2007), *Int. J. Climatol.*, *31*, 633–648.

Fontaine, B., P. Roucou, and P. A. Monerie (2011b), Changes in the African monsoon region at medium-term time horizon using 12 AR4 coupled models under the A1b emissions scenario, *Atmos. Sci. Lett.*, *12*, 83–88.

Fontaine, B., M. Gaetani, A. Ullman, and P. Roucou (2011c), Time evolution of observed July-September sea surface temperature-Sahel climate teleconnection with removed quasi-global effect (1900-2008), *J. Geophys. Res.*, *116*, D041105, doi:10.1029/2010JD014843.

Giannini, A., R. P. Saravannan, and P. Chang (2003), Ocean forcing of Sahel rainfall on interannual to interdecadal time scales, *Science*, *302*, 1027–1030.

Grist, J. P., and S. E. Nicholson (2001), A study of the dynamical factors influencing the interannual variability of rainfall in the West African Sahel, *J. Clim.*, *14*, 1337–1359.

Hagos, S. M., and K. H. Cook (2008), Ocean warming and late-twentieth century Sahel drought and recovery, *J. Clim.*, *21*, 3797–3814.

Janicot, S. (1992), Spatio-temporal variability of West African rainfall. Part I: Regionalizations and typings, *J. Clim.*, *5*, 489–497.

Joly, M., and A. Voldoire (2010), Role of the Gulf of Guinea in the inter-annual variability of the West African monsoon: What do we learn from CMIP3 coupled simulations, *Int. J. Climatol.*, *30*, 1843–1856.

Joly, M., A. Voldoire, H. Douville, P. Terray, and J.-F. Royer (2007), African monsoon teleconnections with tropical SSTs: Validation and evolution in a set of IPCC4 simulations, *Clim. Dyn.*, *29*, 1–20.

Jury, M. K. (2010), Ethiopian decadal climate variability, *Theor. Appl. Climatol.*, *101*, 29–40.

Kalnay, E., et al. (1996), The NCEP/NCAR 40-year reanalysis project, *Bull. Am. Meteorol. Soc.*, *77*, 437–471.

Le Barbé, L., and T. Lebel (1997), Rainfall climatology of the HAPEX-Sahel region during the years 1950-1990, *J. Hydrol.*, *189*, 43–73.

Lebel, T., and A. Ali (2009), Recent trends in the Central and Western Sahel rainfall regime 1990-1997, *J. Hydrol.*, *375*, 52–64.

Leroux, S., and N. M. J. Hall (2009), On the relationship between African Easterly Waves and the African Easterly Jet, *J. Atmos. Sci.*, *66*, 2303–2316.

Losada, T., B. Rodriguez-Fonseca, I. Polo, S. Janicot, S. Gervois, F. Chauvin, and P. Ruti (2009), A multimodel approach to the Atlantic equatorial mode: Impact on the West African monsoon, *Clim. Dyn.*, *35*, 29–43.

Maraun, D., and J. Kurths (2004), Cross wavelet analysis: Significance testing and pitfalls, *Non Linear Processes Geophys.*, *11*, 505–514.

Martin, E. R., C. D. Thorncroft, and B. Booth (2013), The multi-decadal Atlantic SST-Sahel rainfall teleconnection in CMIP5 simulations, *J. Clim.*, doi:10.1175/JCLI-D-13-00242.1, in press.

Mathon, V., and H. Laurent (2001), Life cycle of Sahelian mesoscale convective cloud systems, *Q. J. R. Meteorol. Soc.*, *127*, 377–406.

Mehta, V. M., and T. Delworth (1995), Decadal variability of the tropical Atlantic Ocean surface temperature in shipboard measurements and in global ocean-atmosphere model, *J. Clim.*, *8*, 172–190.

Mohino, E., S. Janicot, and J. Bader (2011), Sahel rainfall and decadal to multi-decadal sea surface temperature variability, *Clim. Dyn.*, *37*, 419–440.

Mohr, K. I., and C. D. Thorncroft (2006), Intense convective systems in West Africa and their relationship to the Africa easterly jet, *Q. J. R. Meteorol. Soc.*, *132*, 163–176.

Monerie, P. A., P. Roucou, and B. Fontaine (2012), Mid-century effects of Climate Change on African monsoon dynamics using the A1B emission scenario, *Int. J. Climatol.*, online doi:10.1002/joc.3476.

Moron, V. (1997), Trend, decadal and interannual variability in annual rainfall of subequatorial and tropical North Africa (1900-1994), *Int. J. Climatol.*, *17*, 785–805.

Newell, R. E., and J. W. Kidson (1984), African mean wind changes between Sahelian wet and dry periods, *J. Clim.*, *4*, 27–33.

Nicholson, S. E., and P. J. Webster (2007), A physical basis for the interannual variability of rainfall in the Sahel, *Q. J. R. Meteorol. Soc.*, *133*, 2065–2084.

Paeth, H., and A. Hense (2004), SST versus climate change signals in West African rainfall: 20th century variations and future projections, *Clim. Change*, *65*, 179–208.

Percival, D. B., and A. T. Walden (2000), *Wavelet Methods for Time Series Analysis*, Cambridge Univ. Press, Cambridge, UK.

Peyrille, P., J. P. Lafore, and J. L. Redelsperger (2007), An idealized two-dimensional framework to study the West African monsoon. Part I: Validation and key controlling factors, *J. Atmos. Sci.*, *64*, 2765–2782.

Pierce, D. W., T. P. Barnett, R. Schneider, R. Saravanan, D. Domenguet, and M. Latif (2001), The role of ocean dynamics in producing decadal climate variability in the North Pacific, *Clim. Dyn.*, *18*, 51–70.

Polo, I., B. Rodriguez-Fonseca, T. Losada, and J. Garcia-Serrano (2008), Tropical Atlantic variability modes (1979–2002). Part I: Time-evolving SST modes related to West African rainfall, *J. Clim.*, *21*, 6457–6475.

Qiu, B. (2003), Kuroshio extension variability and forcing of Pacific decadal oscillations: Responses and potential feedback, *J. Phys. Oceanogr.*, *33*, 2465–2482.

Redelsperger, J. L., A. Diongue, A. Diedhiou, J. P. Ceron, M. Diop, J. F. Gueremy, and J. P. Lafore (2002), Multi-scale description of a Sahelian synoptic weather system representative of the West African monsoon, *Q. J. R. Meteorol. Soc.*, *128*, 1229–1257.

Reed, R., D. Norquist, and E. Recker (1977), The structure and properties of African wave disturbances as observed during Phase III of GATE, *Mon. Weather Rev.*, *105*, 317–333.

Rodwell, M. J., and B. J. Hoskins (1996), Monsoons and the dynamics of deserts, *Q. J. R. Meteorol. Soc.*, *122*, 1385–1404.

Sathiyamoorthy, V., P. K. Pal, and P. C. Joshi (2007), Intraseasonnal variability of the Tropical Easterly Jet, *Meteorol. Atmos. Phys.*, *96*, 305–316.

Smith, T. M., R. W. Reynolds, T. C. Peterson, and J. Lawrimore (2008), Improvements to NOAA's historical merged land-ocean surface temperature analysis (1880-2006), *J. Clim.*, *13*, 538–549.

Stickler, S., and S. Brönnimann (2010), Wind bias of the NCEP/NCAR and Twentieth Century Reanalyses over the West African and Asian Monsoon Regions during the years 1940-1957, ECAC/EMS annual meeting. Zürich, CH, 13-17 September 2010.

Stickler, S., and S. Brönnimann (2011), Significant bias of the NCEP/NCAR and Twentieth Century Reanalyses relative to pilot balloon observations over the West African monsoon region (1940-57), *Q. J. R. Meteorol. Soc.*, *137*, 1400–1416.

Thomas, R. A., and P. J. Webster (1997), The role of inertial instability in determining the location and strength of near-equatorial convection, *Q. J. R. Meteorol. Soc.*, *123*, 1445–1482.

Thorncroft, C. D., H. Nguyen, C. Zhang, and P. Peyrillé (2011), Annual cycle of the West African monsoon: Regional circulations and associated water vapour transport, *Q. J. R. Meteorol. Soc.*, *137*, 129–147.

Torrence, C., and G. P. Compo (1998), A practical guide to wavelet analysis, *Bull Am. Soc Metrol Soc*, *79*, 61–78.

Torrence, C., and P. Webster (1999), Interdecadal changes in the ENSO-monsoon system, *J. Clim.*, *12*, 2,679–2,690.

Tourre, Y. M., B. Rajagopalan, Y. Kushnir, M. Barlow, and W. B. White (2001), Patterns of coherent ocean decadal and interdecadal climate signals in the Pacific Basin during the 20th century, *Geophys Res Lett*, *28*, 2069–2072.

Tourre, Y. M., C. Cibot, L. Terray, W. B. White, and B. Dewitte (2005), Quasi-decadal and interdecadal climate fluctuations in the Pacific Ocean from CGCM. *Geophys Res Lett*, *32*, L07710, doi:10.1029/2004GL022087.

Tourre, Y. M., S. Paz, Y. Kushnir, and B. White (2010), Low-frequency climate variability in the Atlantic basin during the 20th century, *Atmos. Sci Lett*, *11*, 180–185.

Wang, C. (2001), Atmospheric circulation cells associated with the El Niño-Southern Oscillation, *J. Clim.*, *15*, 399–419.

Ward, N. M. (1998), Diagnosis and short-lead time prediction of summer rainfall in tropical North Africa at interannual and multidecadal timescales, *J. Clim.*, *11*, 3167–3191.

White, W. B., Y. M. Tourre, M. Barlow, and M. Dettinger (2003), A delayed action oscillator shared by biennial, interannual, and decadal signals in the Pacific Basin, *J. Geophys. Res.*, *108*(C3), 3070, doi:10.1029/2002JC001490.

Wu, Z., and N. E. Huang (2009), Ensemble empirical mode decomposition: A noise-assisted data analysis method, *AADA*, *1*, 1–41.

Wu, M. L., O. Reale, S. D. Schubert, M. J. Suarez, R. D. Koster, and P. J. Pegion (2009), African easterly jet: Structure and maintenance, *J. Clim.*, *22*, 4459–4480.

Xue, Y., K. M. W. Lau, L. Boone, I. Druyan, S. Seidou, and WAMME team (2012), Evaluation of West African Monsoon processes and feedback: Second WAMME (West African Monsoon Modeling and Evaluation Project) Experiment. 4th AMMA International Conference. Toulouse, FRA, 2-6 July 2012.

Zeng, N., J. D. Neelin, K. M. Lau, and C. J. Tucker (1999), Enhancements of interdecadal climate variability in the Sahel by vegetation interaction, *Science*, *286*, 1537–1540.

Zhang, R., and T. L. Delworth (2006), Impact of Atlantic multidecadal oscillations on India/Sahel rainfall and Atlantic hurricanes, *Geophys Res Lett*, *33*, L17712, doi:10.1029/2006GL026267.